Comparative study between the sliding mode and backstepping current control of a Grid-connected direct drive Wind-PMSG System

Fatiha BEKRAOUI*, Ilhami COLAK**, Amina BEKRAOUI***, Khayra ROUMMANI***, Abdelkader HARROUZ****

*Department of Science and technology, Faculty of Science and technology, Laboratoire de Developpement Durable et d'Informatique (LDDI), Université Ahmed DRAIA, Adrar,ALGERIA.

** Department of Electrical and Electronics Engineering, Nisantasi University, Istanbul, TURKEY.

**** Department of Hydrocarbons and Renewable, Faculty of Science and technology, Laboratoire de Developpement Durable et d'Informatique (LDDI), Université Ahmed DRAIA, Adrar,ALGERIA.

(fat.bekraoui@univ-adrar.edu.dz, ilhami.colak@nisantasi.edu.tr, aminaberkaoui1@gmail.com)

‡ FATIHA BEKRAOUI, ADRAR ALGERIA, Tel : +231 656977654, fat.bekraoui@univ-adrar.edu.dz

Abstract- The object of this paper is to present the efficiency of the backstepping and sliding mode control implemented in a permanent synchronous generator (PMSG) that is directly driven by a wind turbine. To compare the performance of the system using these two control methods. MATLAB/Simulink comparative analysis is performed between the proposed backstepping and sliding mode control methods to compare the performance of the system using these two control methods. The simulation results show that backstepping has a fast dynamic, improved tracking performance, and is more robust than SMC.

Keywords- PMSG; SLIDING MODE CONTROL; BACKSTEPPING; WIND TURBINE.

1. Introduction

In recent years, it has become necessary to generate electric energy from renewable energy sources to reduce pollution from fossil energies. The renewable energy sector is expanding rapidly, with wind technology growing at the fastest rate in the world. Variable speed wind turbines in small wind systems are outfitted with a (PMSG) that is directly ally to the wind turbine. This mechanism is becoming more popular due to its numerous advantages, including low maintenance costs due to the lack of a gear box and slip ring, high strength, low disturbance, rapid dynamic response, and great efficiency [1].

Sliding mode control is indeed a nonlinear controller with a constant dynamic response that ensures system stability by reducing temporary state errors. As the system approaches and remains within the sliding surface, SMC provides durability against parameter changes and external disturbances.

Backstepping Control is a Lyapunov-based nonlinear control. Due to the high efficiency and stability of closed-loop systems, it has recently been extensively studied and adapted to control [2].

This work presents a comparison of the sliding mode control and backstepping on a permanent magnet synchronous generator wind energy system.

Modulization, theoretic research and simulation are providing. The performance of the two controllers was studied and compared in terms of tracking reference, outside noise, and durability versus current sensing failures.

The following is how the paper is structured: The wind energy system-based PMSG is described in Section 1. The two controls are presented in sections 2 and 3. Section 4 deduces the simulation results.

2. WIND ENERGY SYSTEM

2.1. Wind turbine

The expression for power produced by the wind turbine is expressed by [3]:

$$P_m = \frac{1}{2}\rho R^2 V^3 \pi C_P(\lambda,\beta) \tag{1}$$

Where R represents blade length V represents wind speed, ρ signifies air density, and the power coefficient is symbolized by Cp. It is reliant on tip-speed ratio (TSR)and pitch angle; CP is expressed as:

$$C_P(\lambda,\beta) = 0.5\left(\frac{116}{\lambda_i} - 0.4\beta - 5\right)e^{\frac{-21}{\lambda_i}} \tag{2}$$

Subsequently the torque of the turbine is concluded by:

$$T_m = \frac{P_m}{\Omega_r} \tag{3}$$

2.2. PMSG

The model of the generator (permanent magnet synchronous) according to the reference d and q frame of the rotor is the generally used and it is shown as [3]:

$$\begin{cases} V_{sd} = R_s . i_{sd} + \frac{d\varphi_d}{d_t} - \omega_r . \varphi_q \\ V_{sq} = R_s . i_{sq} + \frac{d\varphi_q}{d_t} - \omega_r . \varphi_d \end{cases} \tag{4}$$

$$\begin{cases} \varphi_d = L_d . i_{sd} + \phi_f \\ \varphi_q = L_q . i_{sq} \end{cases} \tag{5}$$

$$\begin{cases} T_{tur} - T_{em} = J.\frac{d\Omega}{dt} + f_c.\Omega \\ T_{em} = \frac{3}{2}.P.[(L_d - L_q) i_{sd} . i_{sq} + i_{sq}.\phi_f] \end{cases} \tag{6}$$

$$\begin{cases} V_{sd} = R_s . i_{sd} + L_d \frac{di_{sd}}{d_t} - \omega_r . L_q . i_{sq} \\ V_{sq} = R_s . i_{sq} + L_q \frac{di_{sq}}{d_t} + \omega_r . L_d . i_{sd} + \omega_r . \phi_f \end{cases} \quad (7)$$

3. SLIDING MODE CONTROL

To overcome torque disturbances, a robust torque controller is proposed using the sliding mode control method. Sliding mode controllers, in general, get excellent tracking performance and robustness to modeling improbability and instability [4].

3.1. The sliding surface.

The S(x) surface represents the desired dynamic behavior of the system that creates the desired closed-loop operation and ensures the convergence of the variable towards the equilibrium point [5-6].

The general equation for determining the surface is:

$$S(X) = \left(\frac{d}{dt} + \delta\right)^{n-1} e \quad (8)$$

$$e = X^{ref} - X, X^{ref} = [x^{ref}, \dot{x}^{ref}, \ddot{x}^{ref}, \ldots]^T \quad (9)$$

With:
e(t) presents the error,
n presents a relation degree,
δ constant,
Xref presents the reference of the signal,
X presents the state of variable.

3.2. Convergence condition

The Lyapunov function indicated the convergence condition by:

$$S.\dot{S} < 0 \quad (10)$$

3.3. Controller design

As soon as the sliding surface and convergence criterion is defined, the order in which the variable to be under control must be returned to the surface and then to the situation of balance during which the sliding modes remain must be fixed.

Consequently, the structure of a controller is split into two parts: one for stabilization one for linearization and.

$$u(t) = u_{eq}(t) + u_n \tag{11}$$

Ueq (t) is the equivalent control derived when the surface derivative is zero:

$$\dot{S}(x) = 0 \tag{12}$$

$$u_n = -K\, sat(s) \tag{13}$$

Where:

K>0

K: the gain of the control.

3.4. Application of the sliding mode control

The controller of the direct current:

$$V_d = \left(\dot{I}_{dref} + \frac{R_s}{L_d} I_d - P\omega_r \frac{L_q}{L_d} I_q\right) L_d + K_d\,.\text{sat}\,(S(i_d)) \tag{14}$$

The quadrature current controller:

$$V_q = \left(\dot{I}_{qref} + \frac{R_s}{L_q} I_q - P\omega_r \frac{L_d}{L_q} I_d + P\omega_r \frac{\varphi}{L_q}\right) L_q + K_q\,.\text{sat}\,(S(iq)) \tag{15}$$

4. Backstepping control

The backstepping controller approach is based on representing looped systems as Lyapunov first-order subsystems. As a result, the system is more resistant to perturbations and more stable overall. The backstepping instruction is a multi-step method in which virtual instruction is produced at every step to guarantee that the system converges to a steady state. The Lyapunov function ensures the stability of each synthesis step [7-8-9].

The following expressions illustrate the errors [9]:

$$\begin{cases} \xi_d = I^*_d - I_d \\ \xi_q = I^*_q - I_q \\ \xi_\Omega = \Omega^* - \Omega \end{cases} \tag{16}$$

The errors are given by:

$$\begin{cases} \dot{\xi}_d = \dot{I}^*_d - \dot{I}_d \\ \dot{\xi}_q = \dot{I}^*_q - \dot{I}_q \\ \dot{\xi}_\Omega = \dot{\Omega}^* - \dot{\Omega} \end{cases} \tag{17}$$

With.

$$\begin{cases} \dot{I}^*_d = 0 \\ \dot{I}^*_q = 0 \end{cases} \tag{18}$$

4.1. Backstepping speed controller

In the first step, by the Lyapunov functions (eq19) a virtual control is created to guarantee the equilibrium state of the system:

$$V_1 = \frac{1}{2} \cdot \xi_{\Omega}{}^{2} \tag{19}$$

The first derivation of Lyapunov function:

$$\begin{cases} \dot{V}_1 = \xi_{\Omega} \cdot \dot{\xi}_{\Omega} \\ = -K_{\Omega} \xi_{\Omega}^2 + \frac{\xi_{\Omega}}{J}\left(-T_{tur} + f \cdot \Omega + K_{\Omega} \cdot J \cdot \xi_{\Omega} + \frac{3}{2} \cdot P \cdot I_q \cdot \varphi_f\right) + \frac{3}{2J} \cdot P \cdot \left(L_d - L_q\right) \cdot I_d \cdot I_q \cdot \xi_{\Omega} \end{cases} \tag{20}$$

With:

$$\dot{\xi}_{\Omega} = \dot{\Omega}^* - \frac{1}{J}\left[T_{tur} - \frac{3P}{2}\left(\left(L_d - L_q\right) \cdot I_d \cdot I_q + I_q \cdot \varphi_f\right) - f \cdot \Omega\right] \tag{21}$$

The first subsystem is stable; the derivative of the norm must always be negative V1 < 0. This translates into the correct choice of stator currents values Id and Iq.

$$\begin{cases} I_d{}^* = 0 \\ I_q^* = -\frac{2 \cdot J}{3 \cdot P \cdot \varphi_f}\left[-k_{\Omega} \cdot \xi_{\Omega} - \dot{\Omega}^* - \frac{C_t}{J} - \frac{f}{J} \cdot \Omega\right] \end{cases} \tag{22}$$

With:

$$\begin{cases} \dot{\Omega}^* = 0 \\ \dot{V}_1 = -K_{\Omega} \xi_{\Omega}^2 \leq 0 \end{cases} \tag{23}$$

4.2. Backstepping voltage controller

In this step, the control voltages Vd and Vq will be calculated based on the virtual entrances of the system. The velocity and current tracking error to obtain the stator voltage references is based on the Lyapunov function:

$$\begin{cases} V_2 = \frac{1}{2} \cdot \left(\xi_d^2 + \xi_q^2 + \xi_{\Omega}^2\right) \\ \dot{V}_2 = \xi_q \cdot \dot{\xi}_q + \xi_d \cdot \dot{\xi}_d + \xi_{\Omega} \cdot \dot{\xi}_{\Omega} = -K_{\Omega}\xi_{\Omega}^2 - K_d \xi_d^2 - K_q \xi_q^2 \end{cases} \tag{24}$$

Using the previous equations, we get.

$$\begin{cases} \dot{\xi}_d = \frac{1}{L_d}\left(R_d \cdot I_d - P \cdot \Omega \cdot L_q \cdot I_q - V_d\right) \\ \dot{\xi}_q = . \frac{2}{3 \cdot P \cdot d \cdot \varphi_f}\left((K_{\Omega} \cdot J - f)\left[T_{tur} - f \cdot \Omega - \frac{3p}{2}\left(\left(L_d - L_q\right) \cdot I_d \cdot I_q + I_q \cdot \varphi_f\right)\right]\right) \\ + \frac{1}{L_q}\left(R_q \cdot I_q + P \cdot \Omega \cdot L_d \cdot I_d + P \cdot \Omega \cdot \varphi_f - V_q\right) \\ \dot{\xi}_{\Omega} = \frac{1}{J}\left[-K_{\Omega} \cdot J \cdot \xi_{\Omega} - \frac{3P}{2}\varphi_f \cdot \xi_q - \frac{3P}{2} \cdot \left(L_d - L_q\right) \cdot I_q \cdot \xi_d\right] \end{cases} \tag{25}$$

The choosing of the Kd and Kq among the positive constants Contributes to system stability.

In the end, the control laws are in the following forms:

$$\begin{cases} I_q^* = -\frac{2 \cdot J}{3 \cdot P \cdot \varphi_f}\left[-k_\Omega \cdot \xi_\Omega - \dot{\Omega}^* - \frac{C_t}{J} - \frac{f}{J}\Omega\right] \\ V_d = -L_d\left(-k_d \cdot \xi_d - \frac{R_d}{L_d} \cdot I_d + \frac{L_q}{L_d} \cdot I_q \cdot \omega\right) \\ V_q = -L_q\left[-k_q \cdot \xi_q - \frac{3 \cdot P \cdot \varphi_f}{2 \cdot J} \cdot c_\Omega - \frac{\varphi_f}{L_d} \cdot \omega - \frac{L_d}{L_q} \cdot I_d \cdot \omega - \frac{R_q}{L_q} \cdot I_q\right] \end{cases} \tag{26}$$

The control designing inputs are:

$$\overline{vd} = R_s \dot{I}_d - L_s p I_q \omega_r + L_q K_d e_d \tag{27}$$

$$\overline{vq} = \frac{2JL_s}{3P\varphi}\left(-\overline{\dddot{\omega}_r} - \frac{B}{J}\dot{\omega}_r - K\omega e_\omega\right) + R_s \dot{I}_q + P(L_s I_d + \varphi)\omega + L_s K_d e_d \tag{28}$$

5. SIMULATION RESULATS

To justify the effectiveness and robustness of the suggested controllers, the following system parameters were used in simulations using MATLAB/Simulink:

Table 1. The permanent magnet synchronous generator parameters.

Criterions	Standards
Poles	3
Rs	1.4(Ω)
Stator L_d inductance	0.0066(H)
J	0.00176[Kg.m2]
Stator L_q inductance	0.0058(H)
F	0.00038[N.m-1]
Flux	0.1546(W)

Table.2 The wind turbine criterions.

Criterions	Standards
ρ	1.225[Kg.m-1]

Friction	0.154[N.m-1]
Radius	3[m]
J (inertia)	0.21[Kg.m2]

A stochastic wind rapidity shape is simulated in this case for comparison of the responses of the recommended controllers to wind speed differences.

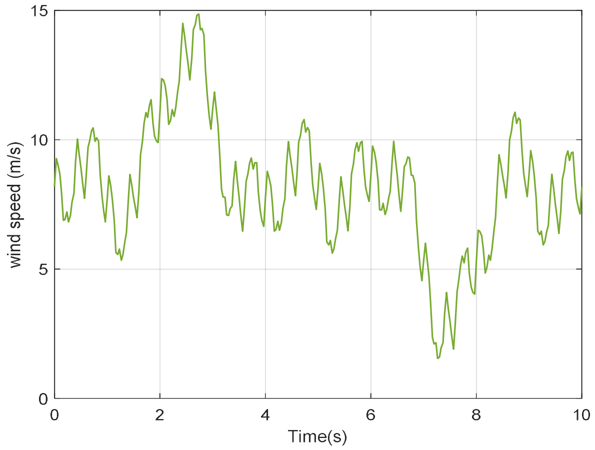

Figure 1. The wind speed (m/s).

The purpose of this test is to know how the two controllers track the reference while assuming the mechanical velocities are equal to their nominal values. Therefore, we can see that the two controllers perform well with respect to reference tracking.

The velocity response of the two proposed control methods is shown in the results. The two suggests follow the reference values with negligible overshoot and ripple, but BSC has a quicker response than SMC and the transient regime imposes is shorter. The proposed controller reduces the SMC's response time from 0.02 seconds to 0.01 seconds.

This result clearly demonstrates that the waves (harmonics) in stator current and torque are greater with SMC than with BSC.

We can conclude that backstepping is more robust than the Sliding mode controller.

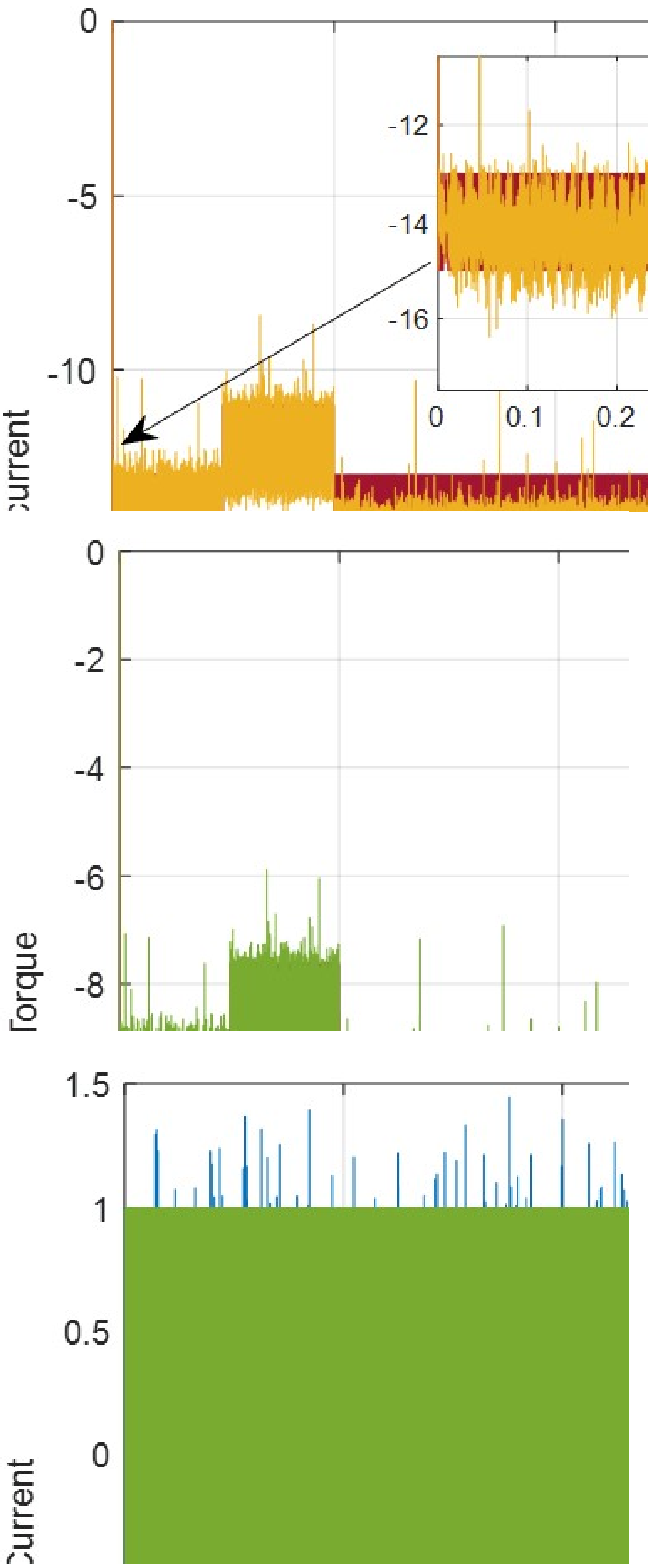

Figure 2. Simulation results under SMC and BSC.

6. CONCLUSION

This paper describes permanent synchronous generator current's control using sliding mode and backstepping control. The park frame generator is used to model the PMSG. Following that, a control strategy utilizing sliding mode first and backstepping second is demonstrated. The simulation results obtainable in this work demonstrate the backstepping control's high efficiency and robustness when compared to the sliding mode method.

References

1. M.Makhad, M.Zazi, "Robust Integral Backstepping control for Optimal Power Extraction of a PMSG-based Variable Speed Wind Turbines", vol. 21. 2014

2. N.Layadi, S.Zeghlache, F.Berrabah, L.Bentouhami, "Comparative Study between Sliding Mode Control and Backstepping Control for Double Star Induction Machine (DSIM) under Current Sensor Faults", 2012-16 International Journal of Information Technology and Electrical Engineering.

3. F. Bekraoui, A. Harrouz, K. Roummani, I. Boussaid ,A. Bekraoui, « PS and GW optimization of variable sliding gains mode control to stabilize a wind energy conversion system under the real wind in Adrar, Algeria », International Journal of Nonlinear Sciences and Numerical Simulation, https://doi.org/10.1515/ijnsns-2022-0237.

4. S.Won Lee, K.Ho Chun, "Adaptive Sliding Mode Control for PMSG Wind Turbine Systems", (http://creativecommons.org/licenses/by/4.0/).

5. L. Hua, F. Xueb , Z. Qinc , J. Shid , W. Qiaod , W. Yangd ,and T. Yang, « Sliding mode extremum seeking control based on improved invasive weed optimization for MPPT in wind energy conversion system », Applied Energy 248(2017), 567-575.

6. S. Bellarbi, D. Saheb Koussa, and A. Djoudi, « Sliding Mode Control for PMSG-based Wind Power System », Physics 1081 (2018), 012012.

7. Y.El Mourabit, A.Derouich, A.El Ghzizal, N.El Ouanjli, O. Zamzoum" Nonlinear backstepping control for PMSG wind turbine used on the real wind profile of the Dakhla-Morocco city", DOI: 10.1002/2050-7038.12297.

8. TAHIRI, F., HARROUZ, A., DUMBRAVA, V., BADOUD, A., & ALNATOOR, M. (2022). NON-LINEAR CONTROLS FOR ROBUSTNESS INVESTIGATION OF PMSG-BASED WIND TURBINE. UPB SCIENTIFIC BULLETIN, SERIES C: ELECTRICAL ENGINEERING AND COMPUTER SCIENCE Учредители: Politechnica University of Bucharest, 84(2), 377-396.

9. M.Ayadi ,N.Derbel, « Nonlinear adaptive backstepping control for variable-speed wind energy conversion system-based permanent magnet synchronousgenerator»,Int J Adv Manuf Technol, Springer-Verlag London2017.